JOURNAL OF NUCLEAR MATERIALS 29 (1969) 82–102. © NORTH-HOLLAND PUBLISHING CO., AMSTERDAM

INTERNAL FRICTION IN ZIRCONIUM-HYDROGEN ALLOYS AT LOW TEMPERATURES

F. POVOLO and E. A. BISOGNI

Departamento de Metalurgia, Comision Nacional de Energia Atomica, Buenos Aires, Argentina

Received 8 July 1968

Using a low-temperature torsion pendulum, internal friction measurements have been performed in polycrystalline wires of high purity zirconium charged with hydrogen up to 56 at %. The internal friction spectrum shows three peaks in the temperature range between —195 and 120 °C. The mechanisms proposed to explain each of the peaks differ fundamentally from those proposed by other authors, and it has been found that the heights of the peaks change with time, even though the hydrogen concentration in the samples remains constant.

A metallographic study of the wires has been made in order to correlate the internal friction results with the distribution and quantity of the several phases in the sample.

En utilisant un pendule de torsion à basse température, des mesures de frottement interne ont été réalisées sur un fil polycristallin de zirconium de haute pureté chargé en hydrogène jusqu'à 56 at %. Le spectre de frottement interne montre 3 pics dans l'intervalle de température —195, +120 °C. Les mécanismes proposés pour expliquer chaque pic diffèrent fondamentalement de ceux proposés par d'autres auteurs et il a été trouvé que la hauteur des pics change avec le temps si la teneur en hydrogène dans les échantillons reste constante.

Une étude métallographique des fils a été réalisée afin de relier les résultats de frottement interne à la distribution et à la quantité des différents phases présentes dans l'échantillon.

Messungen der inneren Reibung wurden an Drähten aus polykristallinem hochreinem Zirkon dotiert mit Wasserstoff bis zu 56 at % durchgeführt. Benutzt wurde die Drehpendelmethode. Das Spektrum der inneren Reibung zeigt drei Peaks im Temperaturbereich zwischen —195 und 120 °C. Zur Erklärung werden Mechanismen vorgeschlagen, die sich wesentlich von jenen anderer Autoren unterscheiden. Es wurde gefunden, dass die Höhe der Peaks sich mit der Zeit bei konstanter Wasserstoffkonzentration ändert.

Metallografische Untersuchungen der Drähte setzen die Messergebnisse in Beziehung zur Verteilung und Menge der verschiedenen Phasen in der Probe.

1. Introduction

The introduction of hydrogen into zirconium fundamentally affects its mechanical properties and since this metal has a wide application in the technology of nuclear reactors, it is important to know the factors that govern the gas-metal interactions in order to understand how this interaction changes the properties of the material. As these changes are governed by processes that occur on the atomic level, and the internal friction of the metal is very sensitive to atomic defects, we have measured the internal friction of various zirconium-hydrogen alloys.

In the following, it will be necessary to refer frequently to the several phases that may appear in the alloy and, since each phase can contribute in a different way to the internal friction, before undertaking the description of the experimental results it is necessary to briefly discuss the zirconium-hydrogen phase diagram.

There are principally two types of phase diagrams for this system: the first one most widely used was proposed by Beck [1]) and the other one by Motz [2]) (fig. 1). Beck, taking into account both his own results and those of other authors, proposed the phase diagram shown in fig. 1a.

The α (hcp) and β (bcc) phases are the two allotropic modifications of pure zirconium [3]). The δ hydride has a fluorite type structure, where the metal atoms have a fcc distribution and the hydrogen atoms occupy the tetrahedral interstitial holes. The γ hydride has a fc tetra-

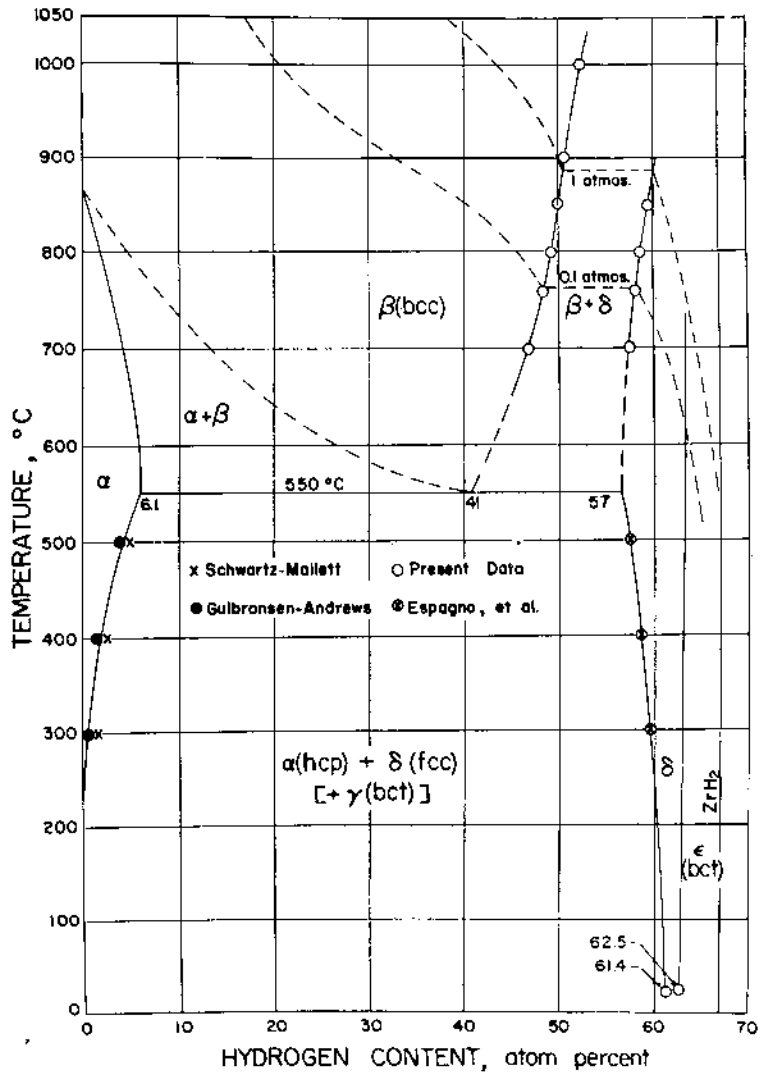

(a)

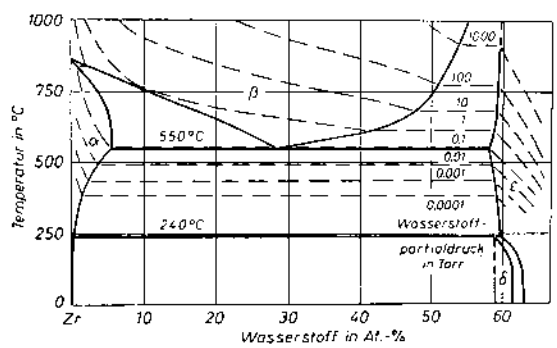

(b)

Fig. 1. Phase diagram for the Zr-H system. (a) according to Beck [1]; (b) according to Motz [2], showing hydrogen isobars.

gonal structure and the only difference from the δ phase is that one of the cell axes is extended with respect to the other two ($c/a > 1$). This phase can alternatively be described as bc tetragonal, since we can go from the bct to the fct cell by multiplying the a parameter by $\sqrt{2}$. Finally, the ε phase is fct like the γ phase, but in this case one of the axes is compressed with respect to the others ($c/a < 1$). This is the only phase whose structure has been studied by neutron diffraction experiments [4, 5]).

Since according to the phase rule, three solid phases (α, δ and γ, fig. 1) cannot coexist at equilibrium, one of the phases, δ or γ, must be metastable. The X-ray [1, 6, 7]), metallographic [6]) and dilatometric [8]) results seem to prove that the γ hydride is the metastable phase. According to Beck [1]) this phase should be a metastable product of the decomposition of the δ phase, that is formed with preference to the equilibrium precipitate, α, on cooling.

Motz [2]) proposed the phase diagram shown in fig. 1b. The main difference with respect to the other authors is the transformation of the ε (tetragonal) hydride to the δ (cubic) hydride that occurs at 240 °C. This implies that the hydride in equilibrium with the α or β phases is not cubic but tetragonal above that temperature. Further discussion of the Zr-H phase diagram is given in ref. [9]).

2. Experimental

For the internal friction measurements we have used a conventional torsion pendulum, fixed at both ends [9]). The pendulum is located in a vacuum chamber whose walls can be cooled with liquid nitrogen, after the system has been filled with hydrogen up to a pressure of about 0.5 Torr, to ensure temperature homogeneity and good heat transfer. (This was desirable because the measurements were made over a range of temperatures down to the boiling point of liquid nitrogen.

The temperature is measured by three thermocouples located near the sample at different heights. During the measurements, the differences between the three thermocouple readings were not greater than 2 °C. To permit the measurement frequencies to be changed an order of magnitude for the activation energies determinations, a recording system was used in which the reflected beam is sent to a photoresistor. The voltage changes across the photoresistor are sent to an amplifier and then to a recording system [9]). All the other curves were taken by reading the amplitude decay on a graduated rule. The samples used were polycrystalline zone-refined zirconium (99.99%) wires of 1 mm diameter and 100 mm long. This material was provided by Atomergic Chemicals Company and a typical analysis is given in table 1.

TABLE 1

Chemical analysis of the zirconium samples

Impurity	(ppm)
Al	<20
Ca	–
Cu	–
Cr	–
Fe	<10
Pb	–
Si	< 5
Ti	–
Mg	–
V	–
Hf	–
C	<20
O	50
H	< 5
N	10
other elements	<10

All wires were previously mechanically polished and then washed with ether in order to ensure a perfectly clean surface. Then they were annealed in high vacuum (10^{-6} Torr) for 1½ h at 750 °C and charged with different amounts of pure hydrogen obtained by passage of commercial hydrogen through a palladium tube. The loading process was made in a Sieverts type apparatus where the sample could be heated in a hydrogen atmosphere and the amount of absorbed gas controlled by

pressure, temperature and time. Almost all of the samples were loaded 1 or 2 h at 750 °C at a hydrogen pressure between 0.1 and 70 Torr.

After the loading, the sample was cooled to room temperature by removal of the furnace. Then it was sealed in a vacuum or in a hydrogen atmosphere in a pyrex or quartz capsule for a heat treatment of 14 h at 400 °C prior to quenching. In order to improve the quenching speed, a weight was arranged so that it broke the capsule when it fell into the quenching liquid (generally alcohol cooled with dry ice). The amount of hydrogen absorbed by each sample was measured, using a hot extraction method, in a Leco apparatus.

Finally, it must be noted that chemical analysis performed on the samples, after they were loaded with hydrogen did not show a further increase in the concentration of other gases over the values given in table 1. The only gas introduced during the loading treatment was hydrogen.

3. Results

3.1. Internal friction

The changes in the internal friction with hydrogen content are shown in fig. 2.

Curve (a) was measured after an annealing of 2 h at 750 °C in vacuum (10^{-6} Torr); there are no maxima. The other curves correspond to the same sample with different amounts of hydrogen and were taken immediately after quenching from 400 °C. A frequency of about 1.6 c/sec was used for all curves. It was impossible to take measurements for higher concentrations because the hydrogen embrittled the wires, and above a certain quantity, the samples cannot be handled. As can be seen, in the temperature range between −195 and 120 °C, the introduction of hydrogen produces three peaks, which we will label P_1, P_2 and P_3 (fig. 3). After removal of the hydrogen by further outgassing at 800 °C for 2 h in high vacuum, curve (a) of fig. 2 was regained.

In order to get each peak, it is first necessary to subtract the background from the measured curves and then separate this peak from the

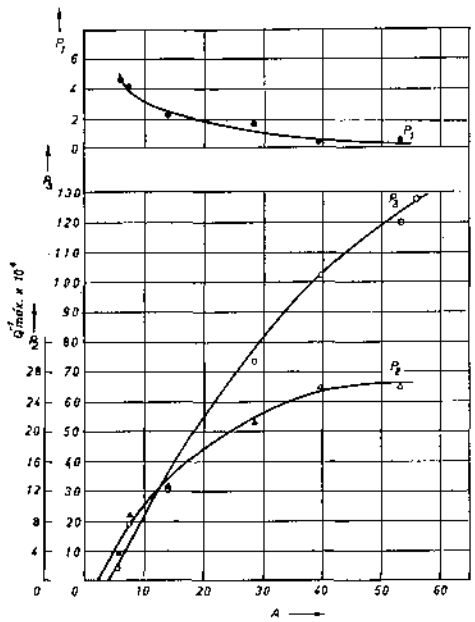

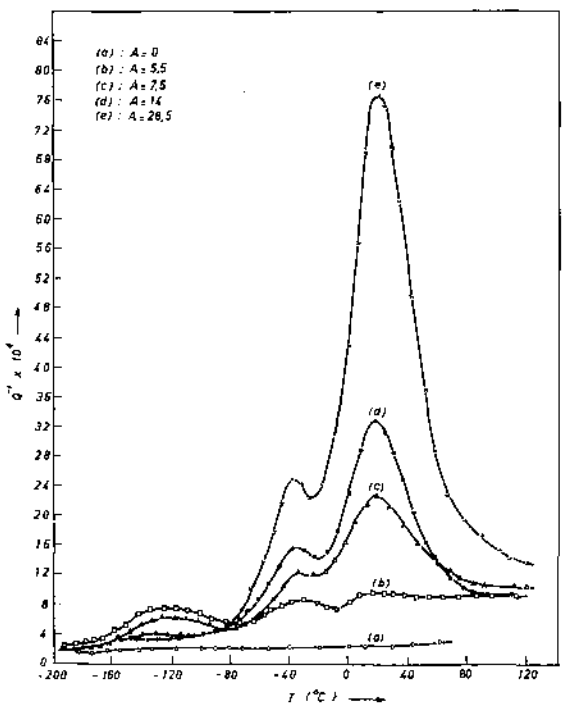

Fig. 2. Dependence of the internal friction on hydrogen content for a sample quenched from 400 °C. A is the hydrogen concentration in at %.

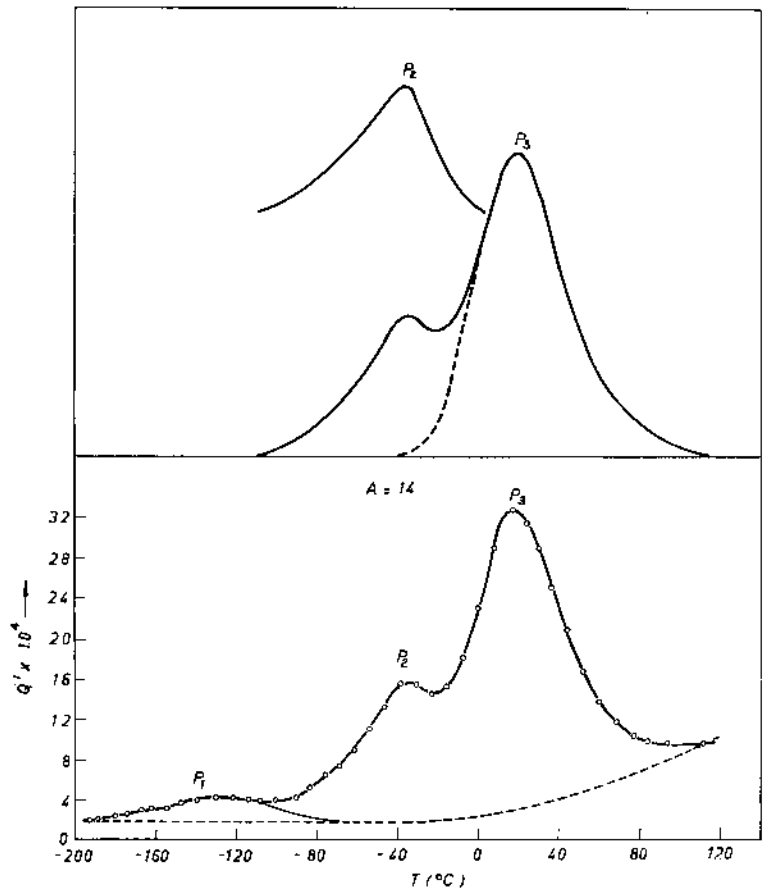

Fig. 3. Criterion adopted to separate the peaks from the measured curves.

others. Unfortunately the background is not constant, since it varies with the hydrogen content, mainly owing to the peaks that appear at high temperatures [10]). Thus, some criterion for the separation must be used that can be justified only by the results it gives. Fig. 3 shows the shape assumed for the background and for the peaks.

From fig. 2 it can be concluded that peak P_1 decreases and peaks P_2 and P_3 increase with the hydrogen concentration in the sample, the last two peaks having different forms of growth. None of the peaks have a linear dependence on the hydrogen concentration. Finally in the temperature range in which the measurements were made, the internal friction was found to be amplitude-independent, at least for maximum surface strains between 6×10^{-5} and 3×10^{-6}.

3.1.1. *Activation energies, frequency factors and shapes of the peaks*

The activation energy and frequency factor for each peak were obtained from the slopes of the $\log \nu_P = \log (\omega_P/2\pi)$ vs $1/T_P$ straight lines [11]) (fig. 4); T_P is the temperature (°K) at which the peak occurs and ν_P the corresponding oscillation frequency.

The calculated activation energies and frequency factors are given in table 2, together with the temperature T at which the peaks will appear for a frequency of 1 c/sec. The last two columns of the table show the measured peak widths at half-maximum and those which might be expected if the peaks were Debye-type (singular) peaks ("theoretical widths"). As can be seen, none of the peaks are singular.

In respect to the shapes of the peaks, it can

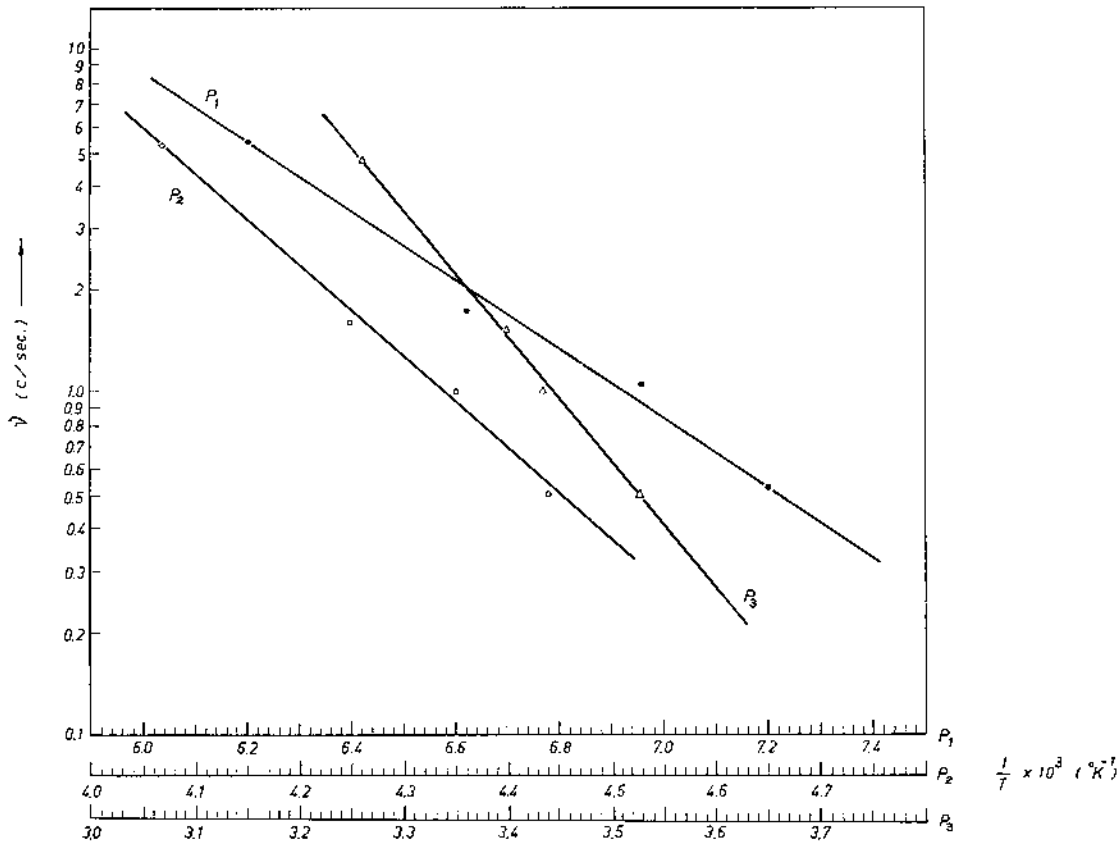

Fig. 4. Shifting of the peak positions with frequency.

TABLE 2

Peak	Q (kcal/mol)	T (°K)	τ_0 (sec)	Width ($°K^{-1} \times 10^3$)	
				theor.	exp.
P_1	4.6 ± 0.5	144	$2 \times 10^{-8 \pm 0.7}$	1.1 ± 0.1	2.6
P_2	12 ± 0.8	230	$6 \times 10^{-13 \pm 0.8}$	0.44 ± 0.04	0.55–0.60
P_3	16.6 ± 0.6	291	$5 \times 10^{-14 \pm 0.5}$	0.32 ± 0.02	0.50

be asserted that P_3 is symmetric when plotted as a function of $1/T$; the other two are slightly asymmetric, but this may be due to the errors introduced in the graphical separation since P_3 is the only well defined peak.

As shown in fig. 3, the plot of Q^{-1} vs T(°C) was preferred over that of Q^{-1} vs $1/T$ (°K^{-1}). The reason is that in the first representation, the P_1 peak and the background are better defined than in the second, although the peaks may be symmetric eventually when plotted as a function of $1/T$ instead of T. In fact, at low temperatures $1/T$ changes very much with a small variation of T, and this makes the lowest temperature peak, P_1, very broad and the other two peaks very narrow, when the internal friction is plotted as a function of $1/T$. In any case, the results obtained with the two representations agree closely.

3.1.2. *Modulus changes*

As the torsional elasticity modulus is pro-

portional to the square of the oscillation frequency, the ratio of the squares of the two frequencies measured at different temperatures, for the same geometrical arrangement, of the same sample, equals the ratio of the two moduli at those temperatures. In fig. 5 the expression $G_T/G_{-190}=\nu_T^2/\nu^2_{-190}$ as a function of temperature was plotted for three different hydrogen concentrations, for the sample to which fig. 2 refers. The change in slope, that must appear in the zone of peak P_1, was not detected in any of the curves. The frequency measurements were taken simultaneously with measurements of internal friction and with a precision of the order of $1/10^3$, which in general is not enough to observe the modulus change associated with a change in relaxation strength of the order of 10^{-4}. The curves of fig. 5 are characteristic of internal friction due to relaxation processes.

3.1.3. *Ageing and recovery of the internal friction*

The heights of the peaks changed with time if, for a constant hydrogen concentration, the sample was maintained at a given temperature. The percentage variations in the heights of the peaks as a function of holding time at 50 °C, for a sample charged at 750 °C, annealed 14 h at 400 °C and quenched, with a hydrogen

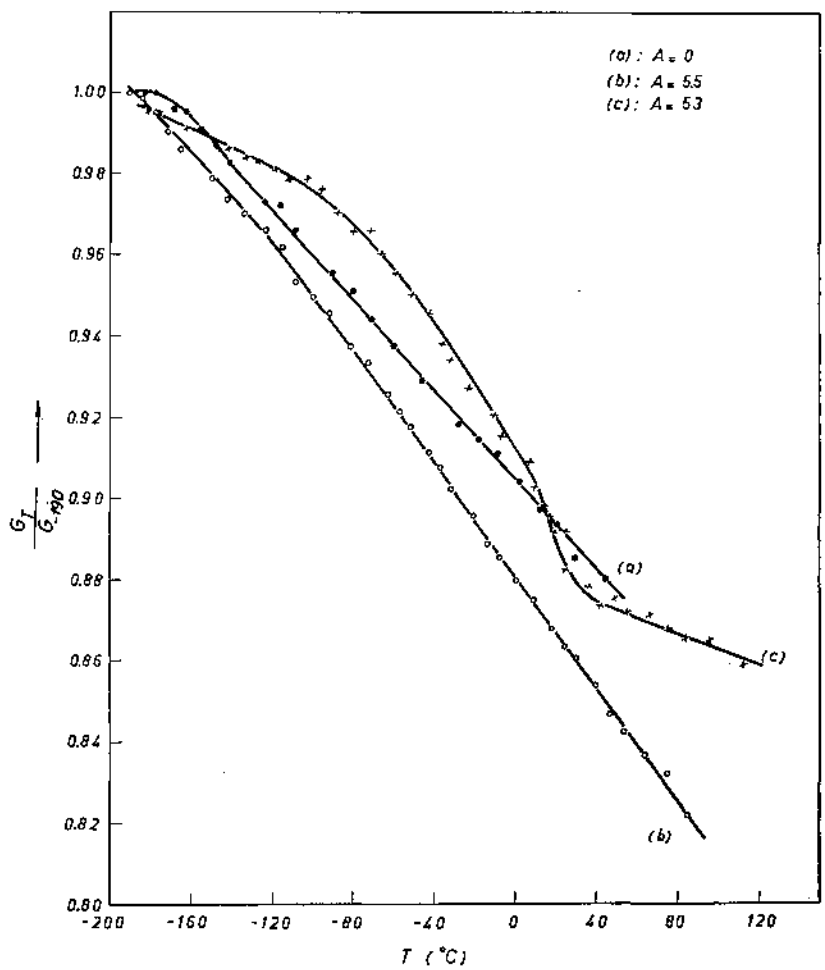

Fig. 5. Elasticity modulus vs temperature for three different hydrogen concentrations. A is the hydrogen concentration in at %.

concentration of 18.5 at % and referred to the state immediately after quenching, are shown in fig. 6. The P_1 and P_3 peaks increase very much and P_2 decreases a little with ageing.

If the aged sample is heated 14 h at 400 °C and quenched, the heights of the three peaks return to their initial values, i.e., the internal friction has recovered. This result is shown in fig. 7; curve (a) was measured after 550 h at 50 °C and (c) after the treatment of 14 h at 400 °C and quenching. Also shown, for comparison, is curve (b) that corresponds to the initial state, i.e., before ageing. There is a full recovery of the internal friction.

Once it has recovered, the internal friction ages again if the sample is kept at a constant temperature, as is shown in fig. 8 for the same sample but maintained at 100 °C. The P_1 peak has increased more than for the ageing at 50 °C even though the initial rates of growth are the same; P_3 has the same rate of increase as for 50 °C and P_2 does not change within the experimental error.

Composition measurements were made during ageing and recovery treatments and no significant changes were found.

In order to measure the activation energies for the ageing processes (assuming they are thermally activated) larger changes in the ageing temperature were taken, since it can be supposed that the change in the ageing rate between 50 and 100 °C may not be easily detectable. Fig. 9 shows the effect of an ageing at 200 °C for another sample with 21 at % hydrogen. Curve (a) was measured after ageing for 236 h at 100 °C and curve (b) after 60 h of ageing at 200 °C. A partial recovery of the internal friction can be observed at this stage. If the temperature is changed to 300 °C, the internal friction recovers still more, curve (c).

If the sample is heated 15 h at 400 °C and quenched, the curve obtained is not much different from that obtained after the treatment of 19 h at 300 °C. In fig. 10 the recovery at 300 °C is compared with that at 400 °C: curve (a) was measured immediately after the quenching from 400 °C, i.e., before the ageing of 236 h at 100 °C; curve (b) [(c) of fig. 9] was obtained

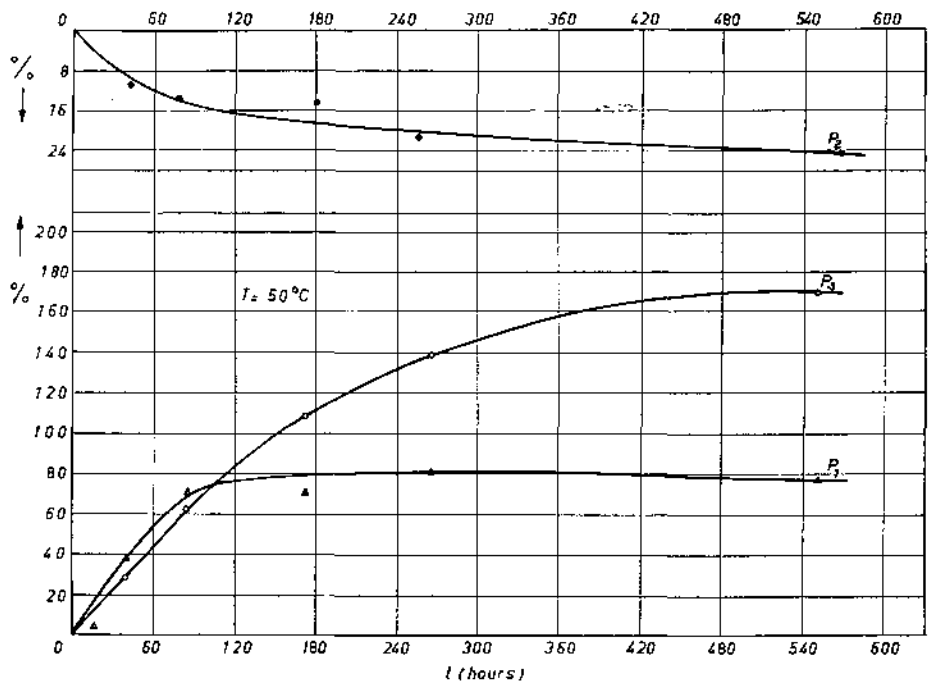

Fig. 6. Percentage variation in the height of the peaks for aging at 50 °C ($A = 18.5$ at % hydrogen).

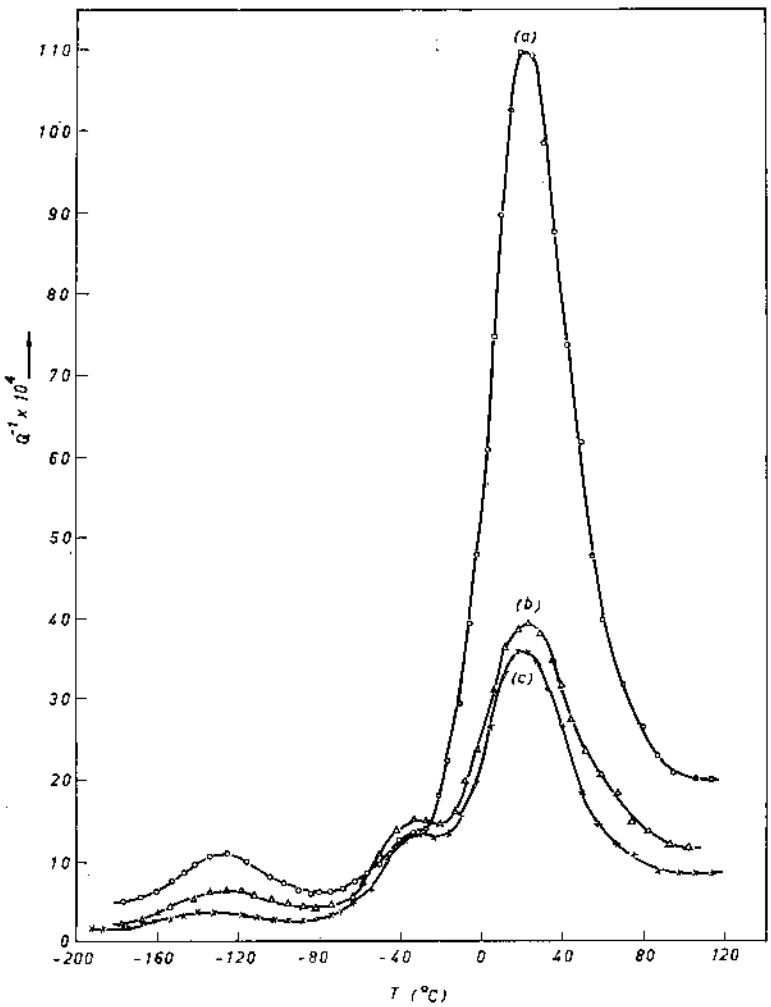

Fig. 7. Recovery of the internal friction by heating at 400 °C. ($A = 18.5$ at % hydrogen); (a) 550 h at 50 °C; (b) initial curve before aging; (c) aged as in curve (a), then annealed 14 h at 400 °C and quenched.

after 19 h at 300 °C, and curve (c) after 15 h at 400 °C and quenching. Therefore, it can be concluded that the treatment at 300 °C almost completely recovers the internal friction and a further heating at 400 °C and quenching does not significantly change the results.

Finally, if the sample after it has been recovered is aged for 80 h at 200 °C, we observe small variations in the heights of the peaks, as can be seen in fig. 11.

From what was just been described and from similar measurements performed on other samples, it can be concluded that:

1. Between room temperature and about 200 °C the internal friction ages; in this temperature range the peaks have small changes and if the ageing is made at lower temperatures in the range, the P_1 and P_3 peaks increase with time and the P_2 peak either decreases slightly or remains constant;
2. Above 200 °C the internal friction does not change significantly with time; if the samples had been aged previously at lower temperatures, the internal friction recovers completely;
3. It was not possible to establish a clear correlation between the internal friction ageing rate and the temperature.

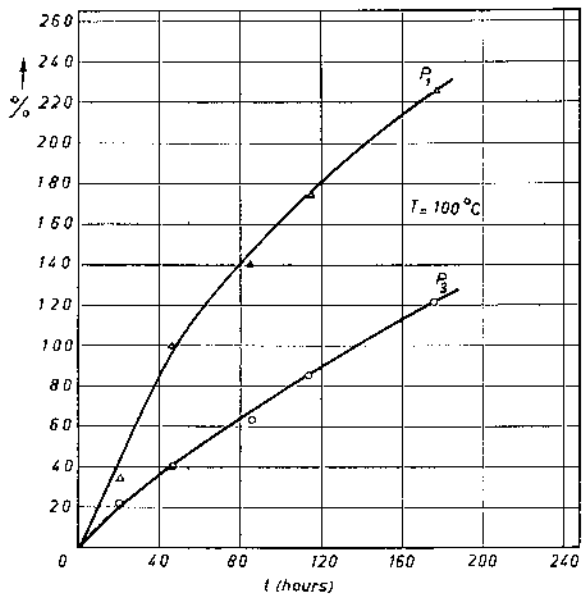

Fig. 8. Influence of aging at 100 °C ($A = 18.5$ at % hydrogen).

3.1.4. *Effect of quenching from different temperatures on the internal friction*

If for a given hydrogen concentration the sample is quenched from different temperatures and the measurements taken immediately after quenching, the P_1 peak increases linearly with the temperature from which the quenching was performed (fig. 12); the P_2 and P_3 peaks do not change within the experimental error. The quenchings were always made from temperatures below the eutectoid temperature (about 540 °C).

In another experiment, in order to determine the influence of the eutectoid transformation on the internal friction curves, the internal friction was measured immediately after charging at 750 °C and cooling to room temperature, and also after ageing for 14 h at 400 °C and quenching. Fig. 13 shows the results for a sample with 15.4 at % hydrogen. As can be seen, there is no significant influence of the treatment at 400 °C [curve (b)] on the results

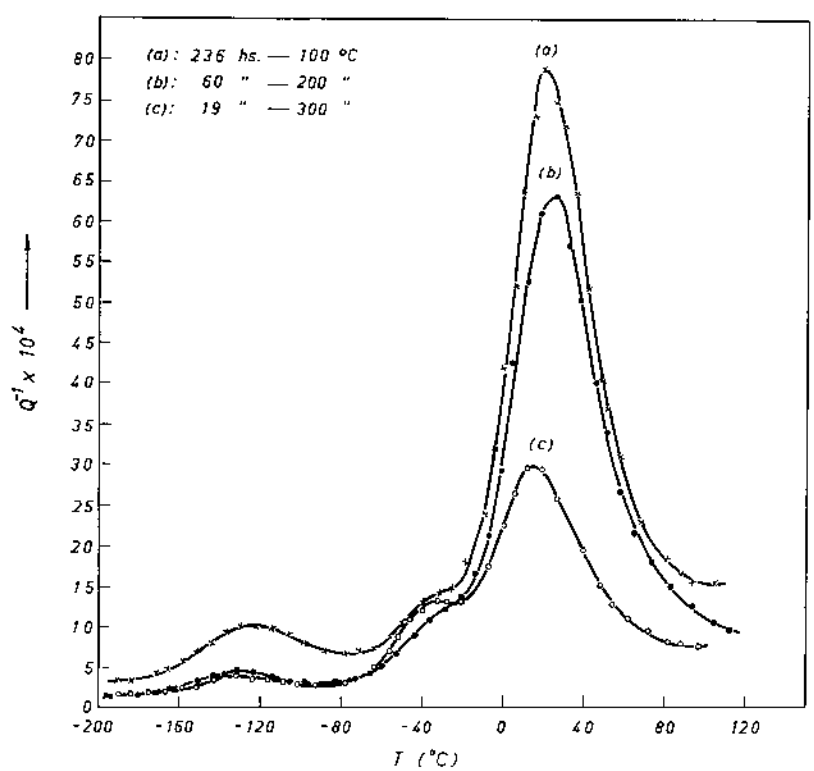

Fig. 9. Recovery of the internal friction by the treatments at 200 and 300 °C ($A = 21$ at % hydrogen).

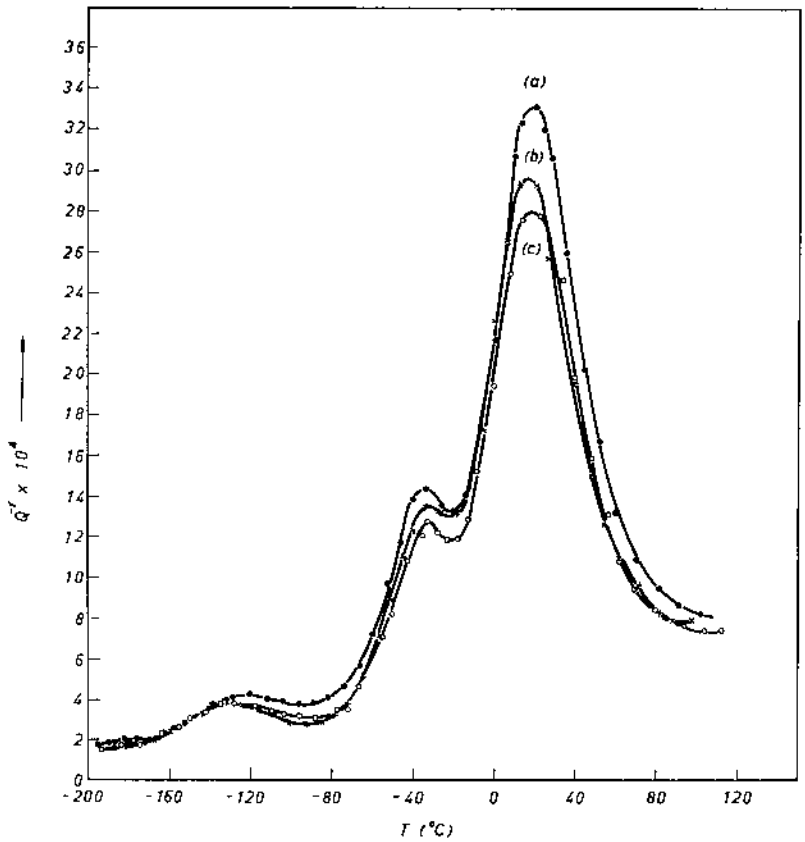

Fig. 10. Effect of the recovery at 300 and 400 °C; (a) initial curve, immediately after hydrogen charging; (b) recovered 19 h at 300 °C; (c) 15 h at 400 °C and quenched ($A = 21$ at % hydrogen).

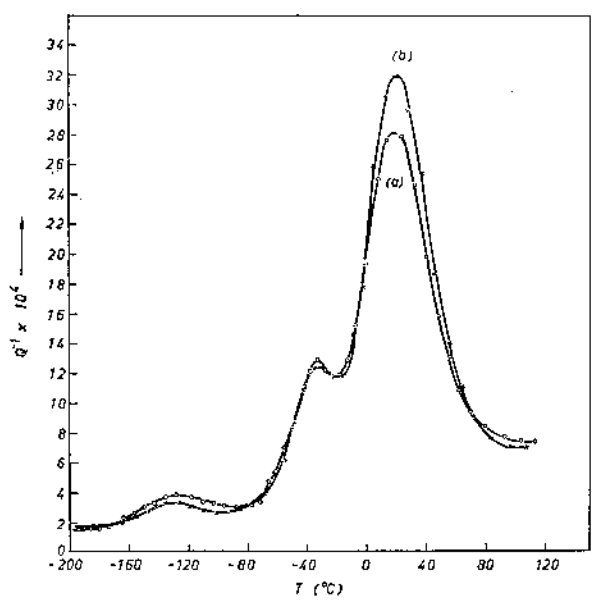

obtained immediately after the charging at 750 °C [curve (a)]. The same effect was observed with other hydrogen concentrations.

Finally, a sample previously annealed in high vacuum at 700 °C was charged with hydrogen *below* the eutectoid temperature. The curves obtained after charging for 4 h at 400 °C and air-cooling, for two hydrogen concentrations, are shown in fig. 14. All three peaks appeared, showing that the eutectoid transformation has no influence on the appearance of the peaks.

3.1.5. *Influence of the deformation*

The P_3 peak increases if the sample previously charged with hydrogen is deformed at room

Fig. 11. Influence of an aging at 200 °C; (a) recovered 15 h at 400 °C and quenched; (b) aged 80 h at 200 °C ($A = 21$ at % hydrogen).

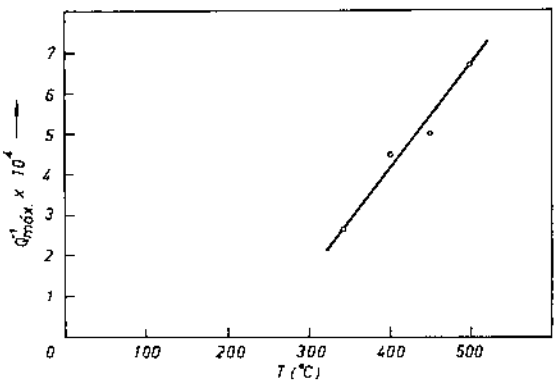

Fig. 12. Variation of the height of the P_1 peak with the temperature from which the sample was quenched ($A = 18.5$ at % hydrogen).

temperature (fig. 15). Curve (a) was measured after charging at 750 °C, annealing at 400 °C and quenching, and curve (b) after deforming the wire 1% by tension at room temperature; the P_3 peak increases noticeably and the other two remain practically the same.

If on the contrary a wire free from hydrogen is deformed, a peak appears in the region of the peak P_1 but no peaks in the region of the other two. This result is illustrated in fig. 15 for a sample deformed 10% in tension at room temperature; the peak is shifted to a slightly lower temperature with respect to the normal P_1 peak. For the three curves of fig. 15, a frequency of 1.3 c/sec was used.

3.2. Metallography

A metallographic study of the wires has been made in order to see how the distribution of the several phases influence the internal friction.

Fig. 16a shows the microstructure of a sample with 1.7 at % hydrogen observed with polarized light. The hydride precipitates appear as

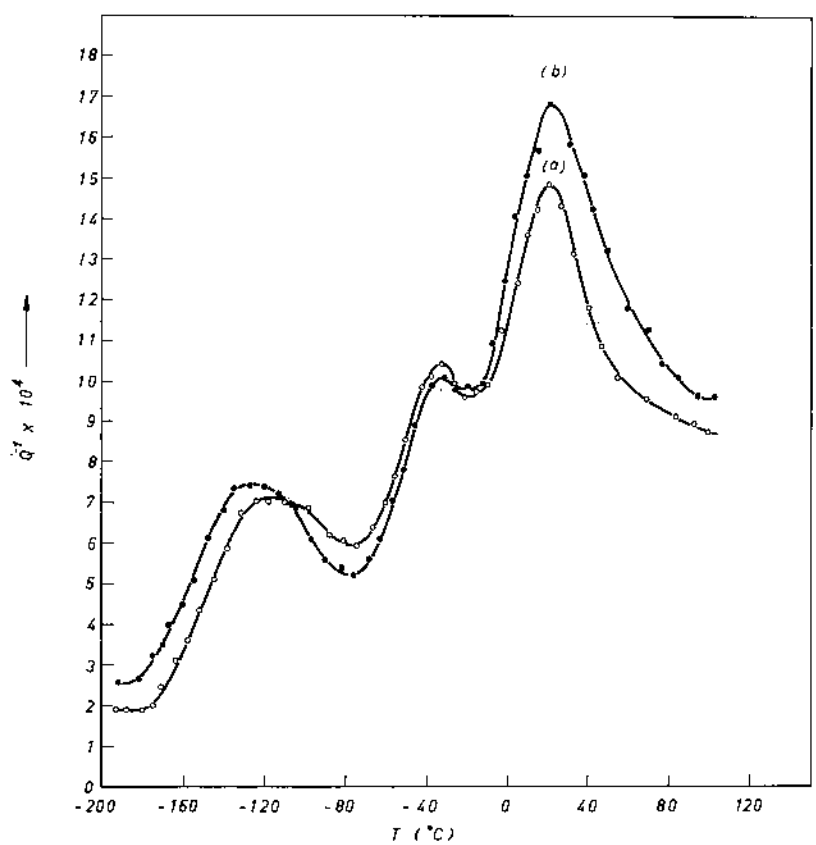

Fig. 13. Influence of annealing at 400 °C on metal charged at 750 °C; (a) charged 1½ h at 750 °C and air-cooled; (b) 14 h at 400 °C and quenched ($A = 15.4$ at % hydrogen).

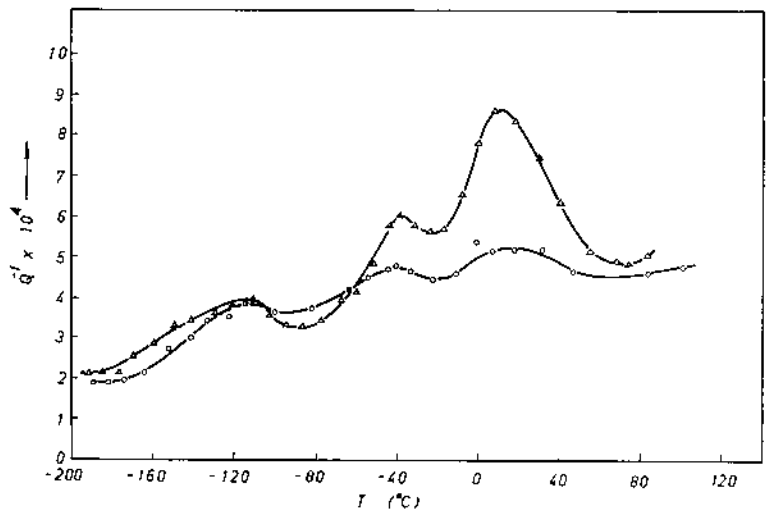

Fig. 14. Influence of charging at 400 °C (4 h) on the internal friction. The curves correspond to a concentration of 2.3 (○) and 7 (△) at % hydrogen.

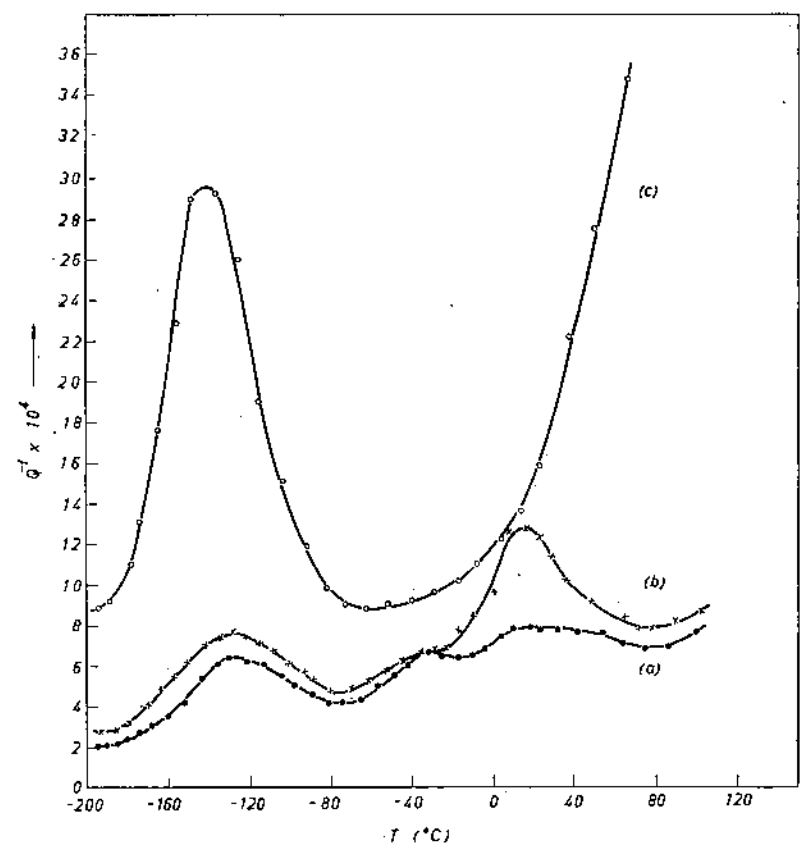

Fig. 15. Influence of the deformation; (a) charged with hydrogen; (b) deformed 1%, $A=3.7$ at % hydrogen); (c) deformed 10%, without hydrogen.

(a)

(b)

(c)

Fig. 16. Shapes and distribution of the hydrides as the hydrogen concentration increases. Notice the needles within the hydrides, especially in (c). (a) $A=1.7$ at %, polarized light; (b) $A=20$ at %, natural light; (c) $A=44$ at %, natural light. $\times 200$

needles in the grains of the hexagonal matrix. This sample was observed after charging at 750 °C and quenching from 400 °C.

On increasing the hydrogen concentration, massive hydrides appear in the matrix and the size of these hydrides increase with hydrogen content, fig. 16 b, c. These pictures were taken with natural light and the matrix appears as a white background.

The form and distribution of the hydrides depend on the hydrogen concentration and how the eutectoid transformation was made.

The needles within the hydrides in fig. 16c correspond to the γ tetragonal phase, which is supposed to be metastable [1, 6].

3.2.1. *Effect of ageing*

Fig. 17 corresponds to the same sample as fig. 16c after an ageing of 6 months at room temperature. Twins within the γ phase can be observed. The background corresponds to the δ hydride.

If the sample of fig. 17 is heated 14 h at 400 °C and quenched, the needles of γ phase decrease in size, increase in number and no longer show twins (fig. 18). Finally if the sample

Fig. 17. Structure of the γ hydride in a sample aged at room temperature ($A=44$ at % hydrogen). Polarized light. $\times 840$

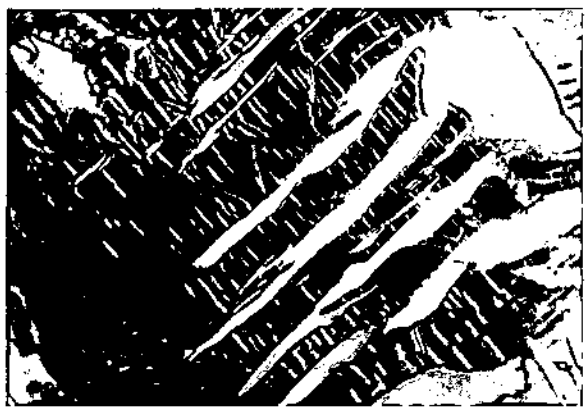

Fig. 18. Structure of the γ hydride in the same sample of fig. 17 but quenched from 400 °C. Polarized light. $\times 840$

Fig. 19. Structure of the γ hydride in the sample of fig. 18 but aged again at room temperature; twins can be detected in the γ phase ($A=44$ at % hydrogen). Polarized light. $\times 840$

is aged again at room temperature (2 months), the needles further increase in size and appear twinned, as is shown in fig. 19. From what was shown and from other experiments made in samples with different hydrogen concentrations, it can be concluded that on ageing, the γ tetragonal phase needles increase in size and become twinned. Annealing at 400 °C and quenching decreases their size, increases their number and, in general, no twins are apparent.

3.2.2. *Effect of the deformation*

If a sample just quenched from 400 °C is deformed in tension at room temperature, the γ phase becomes twinned.

3.2.3. *Effect of the charging at* 400 °C

All the samples studied so far were charged with hydrogen by heating the wires $1\frac{1}{2}$ h at 750 °C, annealing 14 h at 400 °C and quenching. In order to determine the influence of the eutectoid transformation on the formation of the γ phase, metallographic observations were made on a sample charged for 4 h at 400 °C, annealed for 14 h at this temperature and quenched. The needles of the γ phase within the cubic hydride can be seen to be similar to those studied after the 750 °C charging (fig. 20). So it can be concluded that the eutectoid transformation has no influence on the appearance of this phase.

Fig. 20. Presence of γ phase by charging at 400 °C ($A=7$ at % hydrogen). Polarized light. $\times 840$

4. Discussion

Before discussing mechanisms that produce the internal friction peaks, it must be established in what face or interface they occur. In effect, according to the Zr-H phase diagram (fig. 1) at the temperatures and compositions studied, there appear three phases: hexagonal (α), cubic (δ) and tetragonal (γ). As the charging was done at 750 °C it might be supposed that on cooling some β (bcc) phase was retained. However, this is unlikely owing to the fact that the eutectoid transformation is very fast [6]) and that when the sample was charged below the eutectoid temperature, the three internal friction peaks appeared (fig. 14) although in this range of the phase diagram the β phase cannot be formed.

The P_2 and P_3 peaks increase and the P_1 peak decreases with the hydrogen concentration in the alloy (fig. 2); moreover, the P_1 peak tends to vanish for high concentrations. According to the phase diagram, if the hydrogen concentration in the alloy increases, the proportion of hydrides grows (fig. 16) with respect to the matrix. This implies that the P_1 peak cannot be produced by a process occurring within the hydride, but is connected with the α phase or the hydride-matrix interface.

With respect to the P_2 and P_3 peaks, since they increase with the hydrogen content and therefore with the proportion of hydride, it seems reasonable to associate them with the hydrides. There are two hydrides: one cubic and the other one tetragonal. Moreover, the second is always associated with the first, i.e., the tetragonal is always within the cubic and therefore which of the hydrides (or both) contributes to the P_2 and P_3 peak must be determined. In conclusion, from the phase diagram and from the observations on the variations of the heights of the peaks with concentration, it can be concluded that:

a. P_1 has to be associated with the hexagonal phase or the hydride-matrix interface;

b. P_2 and P_3 must be associated with the hydrides.

Each peak will be discussed separately in order to find the process that produces it.

Peak P_1

It might be supposed that this peak is due to a stress-induced diffusion of the hydrogen atoms between the interstices of the hexagonal α phase. In fact, Povolo and Bisogni [12]) have shown that a singular peak can be obtained by a reordering of the hydrogen atoms between the tetrahedral and octahedral interstices by applying a uniaxial tension in the direction of the c axes of the crystal.

Schwartz and Mallet [13]) have found an activation energy of 5.9 kcal/mol for the diffusion of hydrogen in the hexagonal phase. This value is very close to the activation energy for the P_1 peak, i.e. 4.6 ± 0.5 kcal/mol (table 2). Moreover, the height of the peak increases linearly with the temperature from which the sample is quenched (fig. 12); a higher quenching temperature increases the hydrogen in solid solution. Finally, the height of the peak does not change with deformation (fig. 15). There are various results that are in contradiction with this interpretation:

a. The P_1 peak is much wider than a singular peak and the difference cannot be explained even in terms of local distortions of the lattice produced by the hydride precipitates;

b. The P_1 peak height increases during ageing, so either the quantity of hydrogen atoms in the α phase or the proportion of this phase in the alloy must increase. The two possibilities contradict all that is known about the phase diagram;

c. The high value of the frequency factor of the order of 10^{-8} sec (table 2) cannot be associated with atomic jumps, since in that case it would be of the order of 10^{-13} sec.

It might be supposed, too, that the peak is due to hydrogen atom pairs, as has been suggested by Bungardt and Preisendanz [10]) for the P_3 peak. An observation of the hcp structure shows that it is not possible to have a stress-induced ordering of the hydrogen atom pairs

unless the pair is destroyed. Moreover, the maximum hydrogen solubility in this phase, at high temperatures, is of the order of 6 at % (fig. 1) and since there are two tetrahedral interstices for each metal atom, only about 3% of the holes will be occupied by the hydrogen; at room temperature the occupancy will be much less. Under these conditions, the probability of forming a hydrogen atom pair is negligible.

It was shown in fig. 15 that in deforming a hydrogen-free sample a peak appeared in the region of P_1, but slightly shifted (about 15 °C) to lower temperatures. This peak coincides with one measured by Hasiguti et al. [14]) in 99.9% Zr, deformed 80% by cold-rolling, and named P_d by these authors; this peak did not change with room temperature ageing and its characteristics were:

$$Q = 4.1 \pm 0.5 \text{ kcal/mol};$$
$$\tau_0 = 3 \times 10^{-8 \pm 0.5}$$
$$T = 205 \text{ °K (1 kc/sec)}.$$

The P_1 and P_d peaks are compared in table 3.

TABLE 3

Characteristics of the P_1 and P_d peaks

Peak	Q (kcal/mol)	τ_0 (sec)	T °K (1 c/sec)
P_1	4.6 ± 0.5	$2 \times 10^{-8 \pm 0.7}$	144
P_d	4.1 ± 0.5	$3 \times 10^{-8 \pm 0.5}$	126

The P_d peak is believed [15]) to be a Bordoni type peak [16]), i.e. produced by a relaxation process that involves reversible movement of dislocation kinks.

Since P_1 and P_d have similar characteristics, it is reasonable to suppose that they are produced by like processes.

Hasiguti [17, 18]) proposed a model based on the diffusion of kinks trapped by point defects to explain the peaks that appear at slightly higher temperatures than that of the Bordoni peak in several cold-worked pure metals. When the movement of the dislocation is not controlled by kink diffusion, he modified the model and considered trapped dislocation loops. In both models the relaxation strength is given by

$$\Delta = AN\varrho L^2,$$

where A is approximately a constant for a given sample and depends on the temperature, ϱ is the dislocation density, L the length of dislocation line between two nodes and N the number of trapped kinks per unit length of dislocation.

If the P_1 peak is taken to be due to a mechanism of this type, i.e. dislocations trapped by hydrogen atoms, the increase in height during ageing can be explained either as being due to an increase in the dislocation density produced when the hydride precipitates in the matrix, or to a migration of the hydrogen atoms to the dislocation during ageing. Both processes will raise the height of the peak. In this interpretation, however, it is not clear why the height of the peak does not depend on the deformation (fig. 15) and changes linearly with the temperature from which the sample is quenched (fig. 12).

It is impossible at this stage to tell exactly what type of interaction between dislocations and hydrogen atoms produces the P_1 peak since more experimental results are needed on this peak and on the P_d peak. These experiments are in progress in our laboratory.

Finally, it must be pointed out that a similar effect was found by Fanti [19]) in hydrogen-charged palladium. On charging and deforming, or vice versa, the Bordoni peak disappears and another peak is produced at higher temperatures. This peak saturates at very low hydrogen concentrations (5×10^{-4} at %) and for a given deformation, the peak is higher than the Bordoni peak.

The similarity between this peak and the Bordoni peak led Fanti to conclude that both are due to the movement of dislocations near their equilibrium positions and the hydrogen acts as a source for kinks so that the peak is higher than the Bordoni peak. In addition to this, the hydrogen atoms alter the potential

barrier to dislocation movement so that the activation energy is larger than that for the Bordoni peak.

Peak P_2

Bungardt and Preisendanz [10]) measured the internal friction of zirconium wires charged with hydrogen and obtained the P_2 and P_3 peaks but not the P_1 peak. These authors did not observe the ageing effect and did not study the dependence of the height of the peaks on the hydrogen concentration. They believed that the P_2 peak was a singular one and since the measured activation energy was very close to that given by Gulbransen and Andrew [10]) for the diffusion of hydrogen in Zr-H alloys, they attributed this peak to a process that occurs in the hexagonal phase with a mechanism similar to that of the Snoek-peak for bcc metals.

Hasiguti et al. [21]) obtained data for one of the peaks measured in slightly hydrogen-charged Zircaloy-2, which was very close to that of Bungardt and Preisendanz for the P_2 peak. Moreover, since the peak increases with quenching and decreases with annealing, they concluded that this peak is due to the stress-induced diffusion of hydrogen between tetrahedral and octahedral sites and vice versa, in the hexagonal phase.

We disagree with both interpretations since, as was pointed out in the initial part of the discussion, this peak must be due to a process that occurs in the hydrides. In respect to the fact that the activation energy for the diffusion of hydrogen is close to the activation energy of the peak, it must be noted that the value 11.4 kcal/mol given by Gulbransen and Andrew is for the diffusion of hydrogen in the hydrides and not in the hexagonal phase.

The P_2 peak has a width very close to that of a singular peak (table 2). Moreover, the frequency factor is of the order of 10^{-13} sec; its activation energy is close to that of the diffusion of hydrogen in the hydride (12 ± 0.8 kcal/mol and 11.4 kcal/mol respectively) and the modulus decay is typical of a relaxation process (fig. 5). All this leads to the conclusion that this peak is due to the redistribution of the hydrogen atoms within the hydrides.

Chang [22]) made internal friction measurements in a Zr-H alloy in the homogeneity range of the δ phase and did not find peaks. Moreover, as the δ hydride has an fcc structure, applying group-theoretical methods it can be shown [9, 23]) that a preferential redistribution of the hydrogen atoms between the tetrahedral sites cannot be induced by applying external stresses. The P_2 peak must, then, be produced within the tetragonal (γ) hydride.

The cell for the γ hydride is shown in fig. 21. The hydrogen atoms occupy the equivalent positions:

$$(0, 0, 0; \tfrac{1}{2}, \tfrac{1}{2}, \tfrac{1}{2}) + \begin{matrix}(\tfrac{1}{4}, \tfrac{1}{4}, \tfrac{1}{4}); (\tfrac{3}{4}, \tfrac{3}{4}, \tfrac{3}{4}) \\ (\tfrac{1}{4}, \tfrac{3}{4}, \tfrac{1}{4}); (\tfrac{3}{4}, \tfrac{1}{4}, \tfrac{1}{4})\end{matrix}$$

and the metal atoms the center and corners of the cell.

Introducing the jump frequencies between the sites shown in fig. 21 and applying group-theoretical methods [9, 24]), three mechanically active modes appear, supposing occupancy of the tetrahedral interstices only. These modes are shown in fig. 22, together with the relaxation frequencies (λ) and the tension that can excite each mode.

Supposing that the frequencies ω_2 and ω_4 do not differ too much from ω_1 and ω_3 respectively (the c/a ratio is less than 1.1), the relaxation frequencies (or the relaxation times) will not

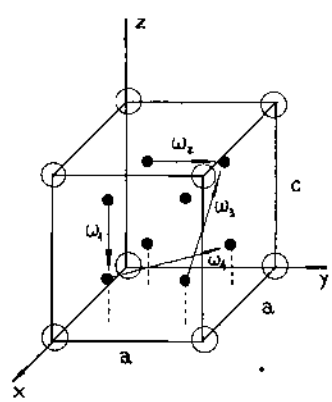

Fig. 21. Cell for the tetragonal hydride. ● hydrogen atom sites.

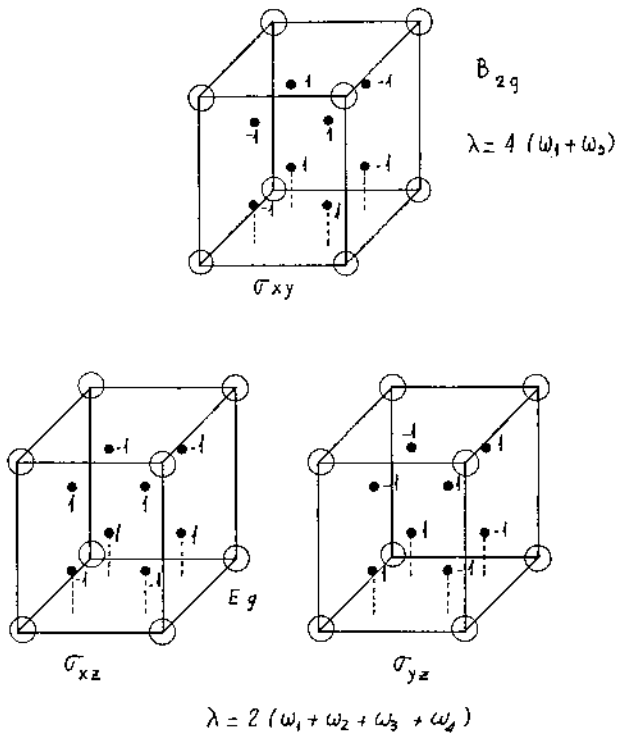

Fig. 22. Mechanical relaxation modes in the γ hydride.

differ greatly for the B_{2g} and E_g modes. As the measured peak will be the superposition of the two modes, it can be expected that its width will not differ too much from that of a singular peak.

In order to make a quantitative estimate of the peak height it is necessary to know the changes of the c and a parameters with the hydrogen concentration in the phase [25]). Unfortunately, there is not much information on the properties of the γ hydride, especially in respect to the composition and the formation mechanism. Some authors assign the formula ZrH to this phase [1]) and others a composition of about 33 at % hydrogen [13, 20, 26]).

Moreover, there are discrepancies in respect to the value of the axial ratio [9]) and it is not known if this depends on the hydrogen concentration in the alloy.

Accepting the model proposed by Beck [1]) for the formation of the γ phase – i.e. as a metastable product of the δ phase on cooling – and admitting the composition ZrH, then from the phase diagram the percentage of γ phase in the alloy can be estimated; this quantity is proportional to that of the δ phase. A plot of the height of the P_2 peak vs the quantity of δ phase (in percent) does not give a straight line but a curve through the origin similar to that of fig. 2. Moreover, with this model the fact that the size of the γ phase needles increases with time during ageing cannot be explained.

Using the phase diagram proposed by Motz [2]) (fig. 1b) and supposing that all the tetragonal phase can be retained when quenching from 400 °C, the peak might increase linearly with the proportion of hydride, at least until near the homogeneity limit (≈ 60 at %) of the tetragonal phase, indicated as ε by this author. This does not happen, as can be seen from fig. 2, since the peak starts to saturate at about 40 at % of hydrogen.

The height of the peak virtually does not change during ageing. So the quantity of γ phase in the alloy must not change very much with time if our interpretation of the process is correct. In fact, from figs. 17 and 18 the values of the ratio: area γ phase/area δ phase (= volume γ phase/volume δ phase) can be estimated in the initial state immediately after quenching from 400 °C and after ageing; the results agree closely.

By taking X-ray Debye-Scherrer diagrams directly of the wires, we have attempted to study the influence of ageing on the structures of the phases that appear in the sample. The experiments were made on aged and recovered samples with a hydrogen concentration between about 15 and 30 at %. Some diffraction lines appeared at low diffraction angles that had not been detected by other authors. The appearance or not of these diffraction lines cannot be clearly correlated to the ageing and recovery. They may correspond to some of the phases already present in the alloy since if we compare the literature data, all authors have not observed the same lines although the X-ray diagrams were taken on powders [1, 2, 6]). These additional lines may indicate, too, that the γ phase changes

its tetragonality with time since they are close to the lines that correspond to this phase.

Peak P_3

This peak must be produced within the tetragonal phase or in the γ-δ interface. The latter possibility can be disregarded if we take into account the fact that P_3 increases (fig. 6) and the γ needles increase in size and decrease in number during ageing (figs. 17 and 18). In conclusion, it can be asserted that this peak must be due to a mechanism that operates in the γ phase.

Chang [22]), in studying the properties of the δ-ε phase transformation, found an internal friction peak for a Zr-H alloy in the homogeneity range of the ε hydride. He attributed this peak to the stress-induced movement of the boundaries of the twins that appear in this phase. The results for the P_3 peak (table 2) with that for Chang's peak in the ε phase are compared in table 4.

TABLE 4

Peak P_3	Peak in the ε phase
$Q = 16.6 \pm 0.6$ kcal/mol	$Q = 20$ kcal/mol
$T = 291$ °K (1 c/sec)	$T = 365$ °K (413 c/sec)
width $= 0.5 \times 10^{-3}$ °K^{-1}	width $= 0.45 \times 10^{-3}$ °K^{-1}
maximum height $= 13 \times 10^{-3}$ (56 at %)	height $= 13 \times 10^{-3}$ (65.8 at %)

Using the expression $\omega\tau_0 \exp(Q/RT) = 1$, the temperature at which the P_3 peak will appear for a frequency of 413 cycles/sec can be calculated; the value is $T = 344$ °K.

As it can be seen, the magnitudes that characterize the two peaks do not differ very much, especially taking into account the fact that some of the data for the ε phase peak were not given by Chang but have been calculated by us from the curves he gave. From the metallographic observations, it is known that the γ phase is twinned and that the amount of twinning increases with ageing and with deformation.

Taking into account these results and the similarity between the P_3 peak and the peak in the ε phase, it can be supposed that the P_3 peak is due to the twins that appear in the γ phase.

It is not possible to make quantitative estimates of the peak height because there is still not a theory of the internal friction peaks produced by twin interface movement, owing to the complexity of the problem. According to Zener [27]), the relaxation is produced because a shear stress across the interface tends to induce movement of this interface, since it adjusts its position in order to minimize the shear stress. This continuous reaccommodation of the interface produces anelastic effects.

Chang [22]), following this idea, attributes the peak in the ε phase to the redistribution of the hydrogen atoms from the distorted tetrahedral interstices in the twin interface to the neighboring octahedral interstices and vice-versa; the twin interface movement is impeded by the redistribution of the hydrogen atoms and is controlled by the hydrogen diffusion rate.

Although the γ phase has an axial ratio $c/a > 1$ and for the ε phase $c/a < 1$, the two hydrides have the same structure and it can be supposed that the mechanism that is acting in ε is valid (naturally with slightly different results) for γ. Moreover, the modulus decreases with a typical form for a relaxation process (fig. 5); the shape of the peak and the frequency factor (of the order of 10^{-13} sec) seem to corroborate the hypothesis that the P_3 peak must be associated with a relaxation process controlled by atomic diffusion and, therefore, supports the idea that the twin interface motion is controlled by the hydrogen.

Finally, Bungardt and Preisendanz [10]) measured for this peak an activation energy of 17 kcal/mol and a width of 0.53×10^{-3} °K^{-1}; these values agree with our results. However, they have attributed this peak to the movement of hydrogen atom pair in the hexagonal phase.

5. Conclusions

The internal friction and metallographic results show that the P_2 and P_3 peaks originate within the hydrides and not (as has been

reported previously in the literature) in the hexagonal phase of zirconium.

The values obtained for the activation energy, width and frequency factor of the P_2 peak together with the changes in the height of the peak with the hydrogen concentration in the sample, show that this peak is produced by the stress-induced migration of the hydrogen atoms within the γ hydride. This interpretation is supported by group-theoretical methods, which show that it is possible to have mechanically active modes for the movement of the hydrogen atoms between interstitial sites within the hydride.

The height of the P_3 peak increases with hydrogen concentration, ageing time and deformation. The metallographic observations show that the γ hydride presents an increasing amount of twinning with ageing and deformation. Moreover, the values of the frequency factor and the activation energy agree closely with those reported for the peak observed in alloys in the homogeneity range of the hydride. This peak is believed to be produced by the movement of the twins that appear in the hydride.

These facts led to the conclusion that the P_3 peak must be associated with the stress-induced motion of the twins in the γ hydride. Finally, from the variation of the P_1 peak with hydrogen concentration, the low value of the frequency factor and the similarities between this peak and the peak obtained in cold-worked high purity zirconium, it can be concluded that the P_1 peak is produced by the interaction between dislocations and hydrogen atoms in the hexagonal phase of zirconium.

Acknowledgements

We are particularly grateful to Ing. D. Vasallo for metallographic techniques and to Mrs. L. Recalde for making the observations. We also wish to thank Ing. J. Maza and Dr. G. Schoeck for many helpful discussions.

This work was performed under the auspices of the Comision Nacional de Energia Atomica, Argentina.

References

1) R. L. Beck, Trans. Am. Soc. Metals 55 (1962) 542
2) J. Motz, Z. Metallk. 53 (1962) 770
3) G. L. Miller, Zirconium (Academic Press Inc., New York, 1957)
4) H. L. Yakel, Jr., Acta Cryst. 11 (1958) 46
5) R. E. Rundle, C. G. Schull and E. E. Wollan, Acta Cryst. 5 (1952) 22
6) D. Whitwham, Mém. Sci. Rev. Mét. 57 (1960) 1
7) J. Vaughan and R. Bridge, Trans. AIME 206 (1956) 258
8) L. Espagno, D. Azou and P. Bastien, Compt. Rend. 247 (1958) 1199
9) F. Povolo, Thesis (University of Buenos Aires, 1967)
10) K. Bungardt and H. Preisendanz, Z. Metallk. 51 (1960) 280
11) B. S. Berry and A. S. Nowick, Physical Acoustics 3A (Academic Press, New York, 1966)
12) F. Povolo and E. A. Bisogni, Acta Met. 15 (1967) 701
13) C. M. Schwartz and M. W. Mallet, Trans. Am. Soc. Metals 46 (1954) 640
14) R. R. Hasiguti, N. Igata and G. Kamoshita, Acta Met. 10 (1962) 442
15) J. Friedel, Dislocations (Pergamon Press, London, 1964)
16) D. H. Niblet, Physical Acoustics 3A (Academic Press, New York (1966)
17) R. R. Hasiguti, Proc. Int. Conf. Crystal Lattic Defects (1962) J. Phys. Soc. Japan 18, Suppl. I (1963) 114
18) R. R. Hasiguti, Phys. Stat. Sol. 9 (1963) 157
19) F. Fanti, Nuovo Cimento 38 (1965) 728
20) E. A. Gulbransen and K. P. Andrew, J. Electrochem. Soc. 101 (1954) 474
21) R. R. Hasiguti, N. Igata, R. Tonomae, Y. Nakamura, N. Sasao and K. Damoto, Symposium on nondestructive testing in nuclear materials 2 (IAEA, Vienna, 1965)
22) R. Chang, J. Nucl. Mat. 2 (1960) 335
23) A. S. Nowick and W. R. Heller, Adv. Phys. 14 (1965) 101
24) A. S. Nowick, Adv. Phys. 16 (1967) 1
25) A. S. Nowick and W. R. Heller, Adv. Phys. 12 (1963) 251
26) R. K. Edwards, P. Levesque and D. Cubiciotti, J. Amer. Chem. Soc. 77 (1955) 1307
27) C. Zener, Elasticity and anelasticity of metals (University of Chicago Press, Chicago, 1948)